1   **Assessing the accuracy of paleodischarge estimates for rivers on Mars**

2   Alexander M. Morgan[1] and Robert A. Craddock[1]

3   [1]Center for Earth and Planetary Studies, National Air and Space Museum, Smithsonian Institution

4

5   Corresponding author: Alexander Morgan (morgana@si.edu)

6

7   **Key points:**

8   • Two methods of estimating martian paleoriver discharge are applied to terrestrial rivers with known

9   bankfull discharges.

10   • The threshold approach yields more conservative discharges when used with realistic grain sizes and high

11   resolution topographic data.

12   • Uncertainties inherent in both methods emphasize the need to consider realistic boundary conditions when

13   applied to Mars.

14

15
16

Abstract

Estimates of river paleodischarges have been used to constrain the former climate of Mars. Paleodischarge has been

calculated using mechanistic approximations of the channel bed shear stress at the threshold of particle motion or

correlative width-discharge relations derived from empirical terrestrial hydraulic geometry data. We apply both

these methods to a study set of gaged terrestrial rivers with field-measured bankfull properties to assess the

reliability of discharge estimates given similar uncertainties as ancient martian rivers. We find that the threshold

method yields conservative values, provided a reasonable grain size is used. However, we find that DEMs of a

similar resolution to those constructed from CTX data may not of sufficient resolution to be useful for estimating

paleohydrologic conditions. Results from our analysis demonstrate the inherent uncertainties when approximating

paleodischarges on Mars and stress the need to consider realistic boundary conditions when determining such

values.

Plain Language Summary

The amount of water, or discharge, that flowed through martian rivers can be used to understand the planet's former

climate. Various methods have been used by researchers to estimate martian river discharge, including relating river

width to discharge or calculating the water volume required to move sediment in the river, but it is uncertain which

of these provide more accurate results. We applied these same methods to rivers on Earth that have field-assessed

flow rates. We find that using grain size yields conservative discharge values, which is generally more desirable, but

that there is significant uncertainty associated with both methods.

1. Introduction

Fluvially formed features on Mars - including valleys, deltas, and alluvial fans - are some of the most

compelling evidence that past conditions were once able to sustain liquid water on the surface. The duration and

timing of these wetter periods remains controversial. Valley networks are not well integrated into the landscape,

having numerous knickpoints along their longitudinal profiles and little dissection on intervalley terrains (Irwin et

al., 2011; Matsubara et al., 2013). Geochemical evidence of substantial aqueous alteration appears to be sparse

(Ehlmann et al., 2011), and some climate models suggest an early Mars that was cold and icy (Wordsworth et al.,

2015), albeit with potentially short lived episodic periods of warming above freezing. However, tributary heads near

45   drainage divides, erosion of topographic highs, and the large volumes of eroded valleys indicate precipitation-fed

46   runoff and an associated hydrologic cycle (Craddock & Howard, 2002; Luo et al., 2017).

47   To ascertain runoff rate, which is a crucial parameter in constraining prevailing hydrologic conditions, one

48   must estimate paleodischarge, the volume of water transported per unit time (expressed in MKS units of m^3/s). Two

49   general approaches have been used (see review in Dietrich et al., 2017). The threshold approach is based on the

50   observation that significant bedload transport does not occur until the channel reaches bankfull discharge (Parker et

51   al., 2007). It is at this threshold value of discharge that larger sediment particles begin to move. Using the bedload

52   grain size diameter - typically the 84th percentile (D_{84}) particle size (which can be a measurement or estimate) - one

53   can approximate flow depth, which when multiplied by a measured width yields discharge. The alternative hydraulic

54   geometry approach uses power law relationships derived for terrestrial rivers that relate channel discharge to channel

55   depth and width, the latter of which can be measured from high resolution images.

56   The threshold approach is physically based but relies on a number of input parameters that are generally not

57   measureable for martian paleorivers. In particular, the grain size distribution, which is a crucial component in

58   estimating both channel depth and bed roughness, cannot be reliably measured from satellite imagery or other

59   remote sensing data (e.g., Presley & Craddock, 2006). Understanding the inherent limitations underlying each

60   method is important for interpreting paleodischarge estimates properly and for understanding the possible

61   implications the estimates have for determining the prevailing environmental conditions at the time of channel

62   formation. This is particularly relevant as plans for current and future robotic spacecraft involve studying fluvially

63   formed environments (e.g., the Gediz Vallis and the Jezero crater delta). We approach this problem by using the

64   same methods that have been used to estimate paleodischarge rates associated with martian river channels and apply

65   them to terrestrial rivers with known bankfull discharges. We begin with an overview of the methods, and then

66   report on discrepancies between discharge estimates and field-determined discharge.

67

68   **2. Methods used for estimating paleodischarge on Mars**

69   *Threshold channel method.* The threshold channel approach uses assumptions of bedload sediment size to

70   approximate the channel depth *H*, which is multiplied by channel width *B* and an estimated velocity *u* to yield

71   discharge *Q*:

72 $$Q = uHB$$ (1)

73 Width is either measured from satellite data or inferred from channel sinuosity wavelength or meander bend radius

74 of curvature (Williams, 1988), while flow velocity is derived using the Darcy-Weisbach equation

75 $$u = \left(\frac{8gHS}{f}\right)^{0.5} \tag{2}$$

76 where g is gravity and S is gradient. f is a coefficient that represents frictional resistance to flow, empirically derived

77 by (Ferguson, 2007) as

78 $$\left(\frac{8}{f}\right)^{0.5} = 17.7\frac{H}{D_{84}}\left[56.3 + 5.57\left(\frac{H}{D_{84}}\right)^{\frac{5}{3}}\right]^{-0.5} \tag{3}$$

79 where D_{84} is the sediment size diameter for which 84% of grains are smaller. The remaining input parameter,

80 channel depth, is not directly measurable from satellite images. It is derived by assuming that significant transport of

81 bedload does not occur until the flow reaches bankfull discharge (Parker, 2008), at which point the bedload shear

82 stress is just above a critical level. The dimensionless Shields parameter τ_{*cr}, describing the initiation of channel bed

83 sediment motion, can be written as

84 $$\tau_{*cr} = \frac{\rho gHS\,a}{(\rho_S-\rho)gD_{84}} \tag{4}$$

85 where ρ_s and ρ are, respectively the density of the sediment and fluid, a represents the sorting of sediment ($D_{84} =$

86 aD_{50}) and is typically ~2 for coarse grained alluvial rivers. The critical shear stress is slope dependent (Lamb et al.,

87 2008; Prancevic et al., 2014):

88 $$\tau_{*cr} = 0.15S^{.25} \tag{5}$$

89 which yields the equation

90 $$H = 0.15S^{-0.75}(P/a)D_{84} \tag{6}$$

91 where P is $\left(\frac{\rho_s-\rho}{\rho}\right)$.

92   Paleodischarge estimates from such physically-derived relationships require input parameters and

93 assumptions about channel gradient S, sediment and fluid density P, and grain size D_{84}. Channel gradient can be

94 obtained from digital elevation models (DEMs) produced from photogrammetry (assuming the local gradient has not

95 been significantly modified relative to the time of DEM production). Sediment density can be safely assumed to be

96 ~3 kg/m^3 (basalt), but fluid density, i.e., the fraction of suspended fine-grained sediment, is not easily determinable.

97 Morgan et al. (2014) approached this by calculating discharges at a range of flow densities from clear water (0%

98 sediment concentration) to extremely turbid hyperconcentrated flows (40% sediment concentration). Likewise, grain

99   size is unknown for any location on Mars except for the exposed Bradbury fluvial conglomerate in Gale Crater

100   (Williams et al., 2013).

101   *Hydraulic geometry method.* An alternative method of calculating discharge is to utilize relations between

102   channel hydraulic geometry and channel forming discharge. Alluvial rivers adjust their geometry in response to

103   various boundary conditions, including flood magnitude, frequency, and sediment load. The channel-forming

104   discharge is "a theoretical discharge that if maintained indefinitely would produce the same channel geometry as the

105   natural long-term hydrograph" (Copeland et al., 2000), and is the discharge that is approximately bankfull, controls

106   channel cross-sectional geometry, and transports more sediment than any other discharge. This discharge generally

107   occurs with a recurrence interval of 1.5 to 2 years (Eaton, 2013; Leopold & Maddock, 1953). Terrestrial datasets are

108   used to derive a relationship between discharge Q and channel width B

109   $$Q = aB^c \tag{7}$$

110   where a and c are coefficients that include all other boundary conditions, including bank strength and flow viscosity.

111   Both of these coefficients show remarkable similarity across terrestrial rivers, such that dataset compilations have

112   been used to estimate terrestrial river discharges of rivers on the sole basis of channel width. When applied to Mars,

113   workers have adjusted a to account for the difference in martian gravity (Irwin et al., 2005; Kite et al., 2015), though

114   analysis of submarine canyons suggest that this may not be necessary (Konsoer et al., 2018). Several datasets have

115   been used to derive a and c through regression analysis. Many martian studies use the relationship derived by

116   Osterkamp & Hedman (1982), who related the active channel width to the two year recurrence discharge, which is

117   often assumed to approximate the channel forming discharge. Jacobsen & Burr (2016) argued that this relation is

118   only correlative and may yield inaccurate discharge estimate values, and argued for the use of hydraulic geometry

119   relationships (e.g. Eaton, 2013) that instead relate bankfull channel width to bankfull discharge.

120

121   **3. Data and methods**

122   We applied both the threshold and hydraulic geometry methods to a set of 110 previously studied, gaged

123   terrestrial river reaches (Table 1) from the western United States. We selected sites that had been surveyed within

124   the past 20 years and that were covered by aerial or satellite imagery during their USGS gage record. These surveys

125   identified bankfull dimensions by topographic indicators (e.g. shift from near-vertical bank to horizontal flood plan)

126   and determined bankfull discharge by comparing bankfull depth to USGS gage data or through modeling. Two of

127   these surveys reported median bedload grain size measured by Wolman count. We used sites in the western United

128   States because (1) less vegetation makes the channels easier to map, (2) the lower level of human development

129   relative to the eastern United States limits the impact of anthropogenic factors on river geometry, and (3) the

130   prevailing climate on Mars during the time of major fluvial modification is believed to be arid to semi-arid (Barnhart

131   et al., 2009). To further avoid human impact, we utilized the National Inventory of Dams (USACE, 2016) to avoid

132   sites that were immediately upstream or downstream of a dam.

133   We measured river widths at 1:1000 scale, mapping up and downstream from each gage and stopping at

134   any confluences or branches with National Hydrogeography Database water bodies (which includes both natural and

135   artificial features). As the discharge estimate methods discussed above are only valid for alluvial rivers, we avoided

136   areas where it was uncertain whether the channel may have been a bedrock channel. The mapped river reach

137   distance therefore varied, but in almost all cases was at least 500 m.

138   As a basemap we utilized image data from the Esri visual imagery layer and the National Aerial Imagery

139   Program (NAIP). The Esri visual imagery layer is a mosaic of satellite image data with resolution of 30-50 cm/pixel

140   while NAIP photographs have a spatial resolution of 1 m/pixel and temporal resolution of 3-5 years since 2003. The

141   spatial resolution of both datasets is thus approximately equal to images returned by the HiRISE camera (McEwen et

142   al., 2007). Unlike dry martian channels, channel edges in our dataset could be difficult to map due to exceptionally

143   high or low flow on the image acquisition date. We therefore used the image that was taken on a day with a

144   discharge closest to the field-assessed bankfull discharge. Elevations used for the threshold method were obtained

145   from the 10 meter national USGS DEM, which is similar in resolution to DEMs derived from CTX (Malin et al.,

146   2007) stereo pairs.

147   Bankfull widths were generally easy to identify by the water edge, channel bars, or vegetation. We

148   excluded areas where dense vegetation made it impossible to map channel edges. For each site we obtained a

149   distribution of channel widths, and derived an average width with confidence intervals. We then calculated bankfull

150   discharge using the threshold approach (Equations 1 – 6) and the hydraulic geometry approach (Equation 7). Our

151   coefficients for Equation 7 came from the compilation of Eaton (2013), which has previously been used for

152   estimating discharge within martian rivers (Jacobsen and Burr, 2016; Kite et al, 2015, 2019).

153   Because grain size cannot be reliably measured from high resolution satellite imagery, we assumed that the

154   channels were gravel bedded, and for the threshold approach calculated discharges using a range of 4 mm (fine

155 gravels) to 64 mm (very coarse gravels). For the two datasets that included grain size distribution from Wolman

156 counts (Lawlor, 2004; Moody et al., 2003) we also calculated the discharges using the known grain size.

157

158 **4. Results and discussion**

159   Channel width measured from remote sensing imagery was generally close to the bankfull widths reported

160 in the literature (Fig. 1). While in some cases there was some deviation from the field reported width, this is likely

161 less of a difference than would be obtained from measuring martian channels that have been subjected to billions of

162 years of erosion. The strong agreement between field and remote sensing obtained width gives a higher degree of

163 confidence in our calculated discharge estimates.

164   The discharges computed using both the threshold (Fig. 2) and the hydraulic geometry (Fig. 3) methods

165 have a large scatter, indicative of the inherent uncertainties when attempting to estimate paleoflow solely from

166 remote sensing observations. The hydraulic geometry approach gave discharge estimates that were reasonably close

167 to the reported bankfull discharges. In their assessment of paleodischarge accuracy, Jacobsen & Burr (2016) argued

168 that due to the use of "correlative" (e.g. Osterkamp & Hedman, 1982) over "causal" (e.g. Eaton, 2013) relationships

169 in estimating martian channel paleodischarge, flow rates for larger (>90 m width) channels may have been

170 underestimated while those for smaller (<60 m width) channels may have been overestimated. As most of these

171 larger channels have been dated to the Noachian-Hesperian, and smaller channels to the Hesperian-Amazonian, this

172 would indicate a greater contrast in discharges during these two eras and that the decline in martian fluvial activity

173 was more extreme than previously recognized. While true that the differing coefficients between these relations will

174 result in increasingly contrasting discharge estimates for large and small channels, we find that the projected trend

175 line for the Eaton (2013) relationship actually deviates considerably more from the field-reported discharge than the

176 Osterkamp & Hedman (1982) relationship. These relations are derived from rivers in different physiographic regions

177 – Osterkamp & Hedman (1982) only used rivers in the Missouri river basin while Eaton (2013) used a dataset that

178 mostly consisting of rivers in the western United States and Canada, but also the United Kingdom, China, and New

179 Zealand. Even so, this indicates that the discharges calculated using the "causal" relation, as argued for by Jacobsen

180 & Burr (2016) may actually be less accurate than those originally obtained using the "correlative" relationship.

181 Regardless, the large scatter in data points using both methods reveals the significant uncertainty in using either of

182 these relationships even when applied to terrestrial rivers. It is uncertain how applicable hydraulic geometry

183   relationships derived for rivers on Earth are when applied to martian rivers. A gravity correction is commonly

184   applied, but other boundary conditions, such as bank strength or relative sediment supply, are not well constrained

185   for martian rivers. Therefore the greater contrast in Noachian-Hesperian and Hesperian-Amazonian discharges

186   reported by Jacobsen & Burr (2016) is not well supported by our analyses.

187   The threshold approach generally underestimated the reported bankfull discharge. The coarsest grain size

188   used (64 mm) yielded results that were closest to the reported bankfull discharge, but this value deviated

189   considerably for the channels with higher discharge. It is possible that our assumption of the study sites being gravel

190   bedded was incorrect. However, the datasets with field measured grain sizes from Wolman counts (Lawlor, 2004;

191   Moody et al., 2003) also underestimated the reported bankfull discharge. This indicates that the threshold approach

192   provides conservative values, which makes it desirable for obtaining discharges to be used in evaluating Mars' past

193   hydrologic conditions. However, this comes with two important caveats. First, we found that using the USGS 10 m

194   DEM added large uncertainty to our results (Fig. 3) compared with the presumably more accurate gradients obtained

195   from field measurements. 10 meters is larger than the scale of many channel features such as pool and riffle

196   sequences. In addition, errors of just several meters in altitude could have a significant impact on the computed

197   gradient. This means that digital elevation models derived from CTX stereo pairs may not be of sufficient resolution

198   to derive paleodischarge estimates. Indeed, Wang & Wu (2016) demonstrated that even after co-registering CTX

199   and HiRISE DEMs there can be altitude discrepancies of up to tens of meters. This emphasizes the need for HiRISE

200   resolution images to derive topographic data. Second, these results indicate that it is crucially important that realistic

201   grain sizes are selected as input parameters. Grain size cannot be obtained from remote sensing imagery. Martian

202   channels are generally assumed to be gravel bedded (Dietrich et al., 2017; Kite et al., 2015, 2019; Morgan et al.,

203   2014; Palucis et al., 2014), but the specific choice of input grain size has a major effect on the computed discharge

204   estimate. A well-defined grain size distribution of fluvially transported sediment is only known for the Bradbury

205   fluvial conglomerate in Gale crater (Williams et al., 2013), but the broader context (e.g. the width and gradient of

206   the channel that deposited the grains) is unknown. Previous workers have used a range of values as an input grain

207   size. Wilson et al. (2004) used rocks at Viking and Pathfinder landing sites to obtain a D_{84} of 164 mm for estimating

208   outflow channel discharge, Kleinhans et al. (2010) assume 100 mm for a channel feeding a fan delta, Morgan et al.

209   (2014) interpret HiRISE texturing to get a D_{50} of 125-250 mm on an alluvial fan surface, and Howard et al. (2007)

210   use meter scale boulders visible in HiRISE images of a delta. The use of large grains visible in HiRISE images can

211   be problematic, as demonstrated by a case study at the Truckee River (Fig. 4, 10 km upstream from gage 10350340).

212   Large boulders several meters across are visible in Digital Globe images as well as in Google Street View imagery.

213   When used as values for the bedload D_{84}, we calculate discharge estimates of 15,000 m^3s^{-1}, which is approximately

214   equal to that the median flow of the Mississippi River at Baton Rouge (gage 07374000), and several orders of

215   magnitude larger than the maximum recorded discharge (during 22 water years of record) on the Truckee River.

216   Using these grain sizes to approximate discharge, as has been done for martian rivers, would result in a severe

217   overestimate. It is possible that these boulders were carried into the channel by landslides or debris flows from

218   nearby hills and will not be transported downstream until they are broken down into smaller particles. Similarly,

219   boulders observed in HiRISE images may have been transported to the location by processes other than fluvial

220   bedload transport, or could be blocks formed by cementation of emplaced sediment after deposition.

221   The maximum channel width used in our analysis was 215 m, which is narrower than many identified

222   martian paleochannels, including those studied by Irwin et al. (2005) (20 separate channels, mean width 352 m) and

223   Raumann et al. (2005) (3 profiles along one channel, mean width 445 m). Ancient narrow channels on Mars are

224   relatively rare, though this could be an effect of the difficulty in preserving small-scale features subject to impact

225   gardening or aeolian modification. In a global survey for more recent (and presumably better preserved) Amazonian

226   rivers, Kite et al. (2019) measured 205 channels, most being between 50-100 m in width. It is important to note that

227   channels will be far narrower than their enclosing valleys, which on Mars can extend up to 20 km in width. In the

228   absence of high resolution image data, early workers (e.g. Weihaupt, 1974) used valley width as a proxy for channel

229   width, resulting in excessively large discharges. The sparse distribution of preserved channels continues to be a

230   challenge for constraining runoff rates on early Mars.

231

232   **5. Conclusions**

233   The high uncertainties inherent in estimating martian paleodischarge demonstrate the need to consider all

234   available boundary conditions and to treat results as order of magnitude approximations. Given the use of realistic

235   grain sizes, the threshold approach provides conservative values, which are generally more desirable. The high

236   amount of scatter from both methods emphasizes the need for careful interpretation of paleodischarge estimates on

237   Mars. Results should be assessed with other boundary conditions, such as realistic source area runoff rates and

238   timescales of downslope basin fill, and be considered order of magnitude approximations.

239

240

241

Acknowledgements

Table and Figures

Table 1: Data sources used for the analyses

| Data source (# of sites)	Region	Grain size (mm)	Channel bankfull width (m)
Dutnell, 2000 (36)	Kansas; Missouri; Oklahoma; Texas	N/A	12 - 215
Castro & Jackson, 2001 (39)	Oregon; Washington	N/A	11 - 182
Moody et al., 2003 (29)	Arizona; New Mexico	0.1-160	5 - 56
Lawlor, 2004 (6)	Western Montana	5-215	6 - 23

252

253

254

Figure 1. Comparison of the literature-reported bankfull channel width with the channel width as measured from

remote sensing images. The shaded grey area indicates the 95% confidence interval In general, our measured widths

are a close match to the actual bankfull widths measured in field surveys.
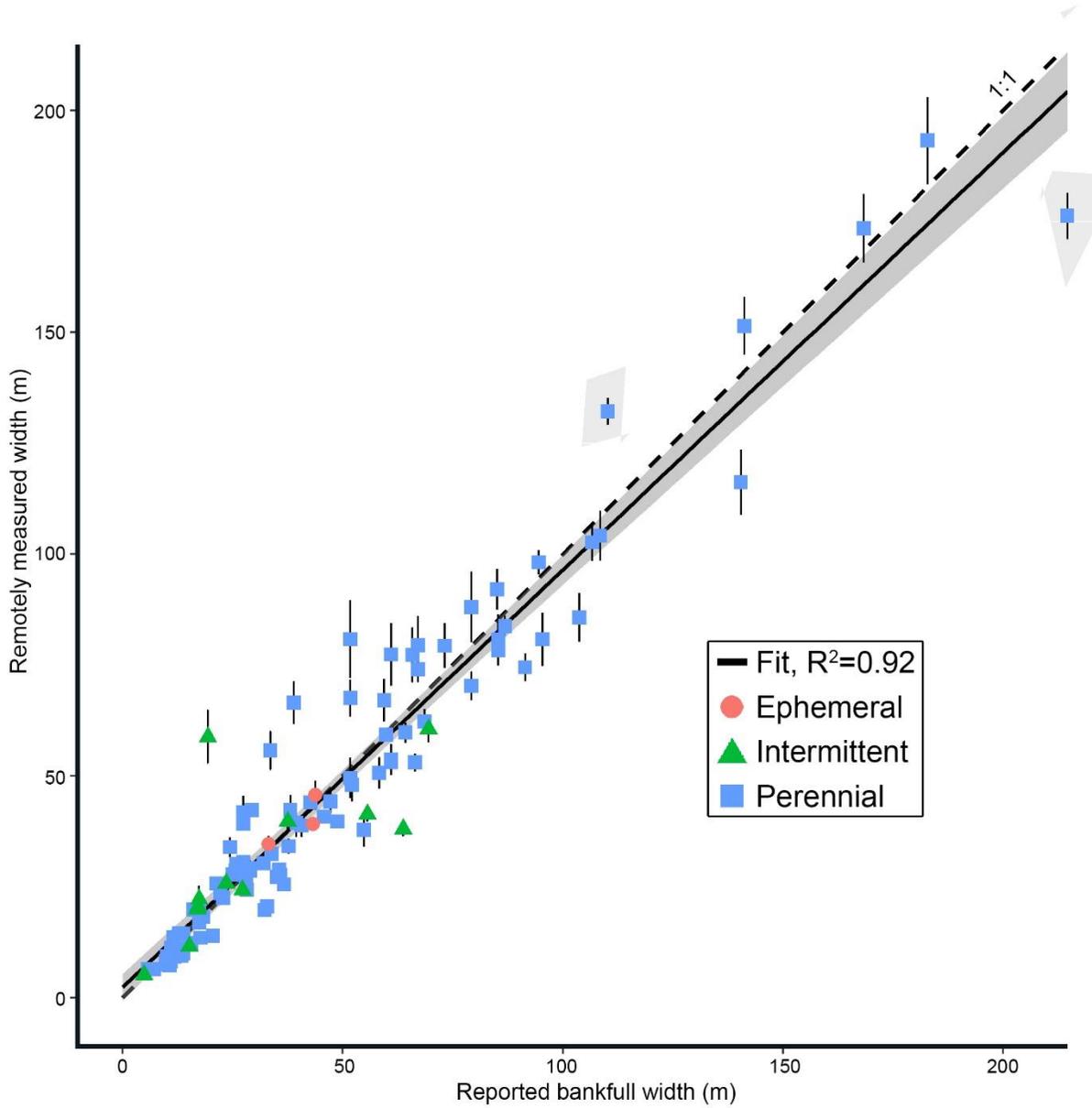
262   **Figure 2.** Discharge estimate results using the hydraulic geometry method. Colored lines are regressions based on

263   each relationship. Black line indicates a 1:1 relation between the reported and estimated bankfull discharge. There is

264   significant scatter from both of the hydraulic geometry correlative relationships, though the trend line for the older

265   Osterkamp and Hedman (1982) relation yields results closer to the field-assessed discharge than the Eaton (2013)

266   relation.
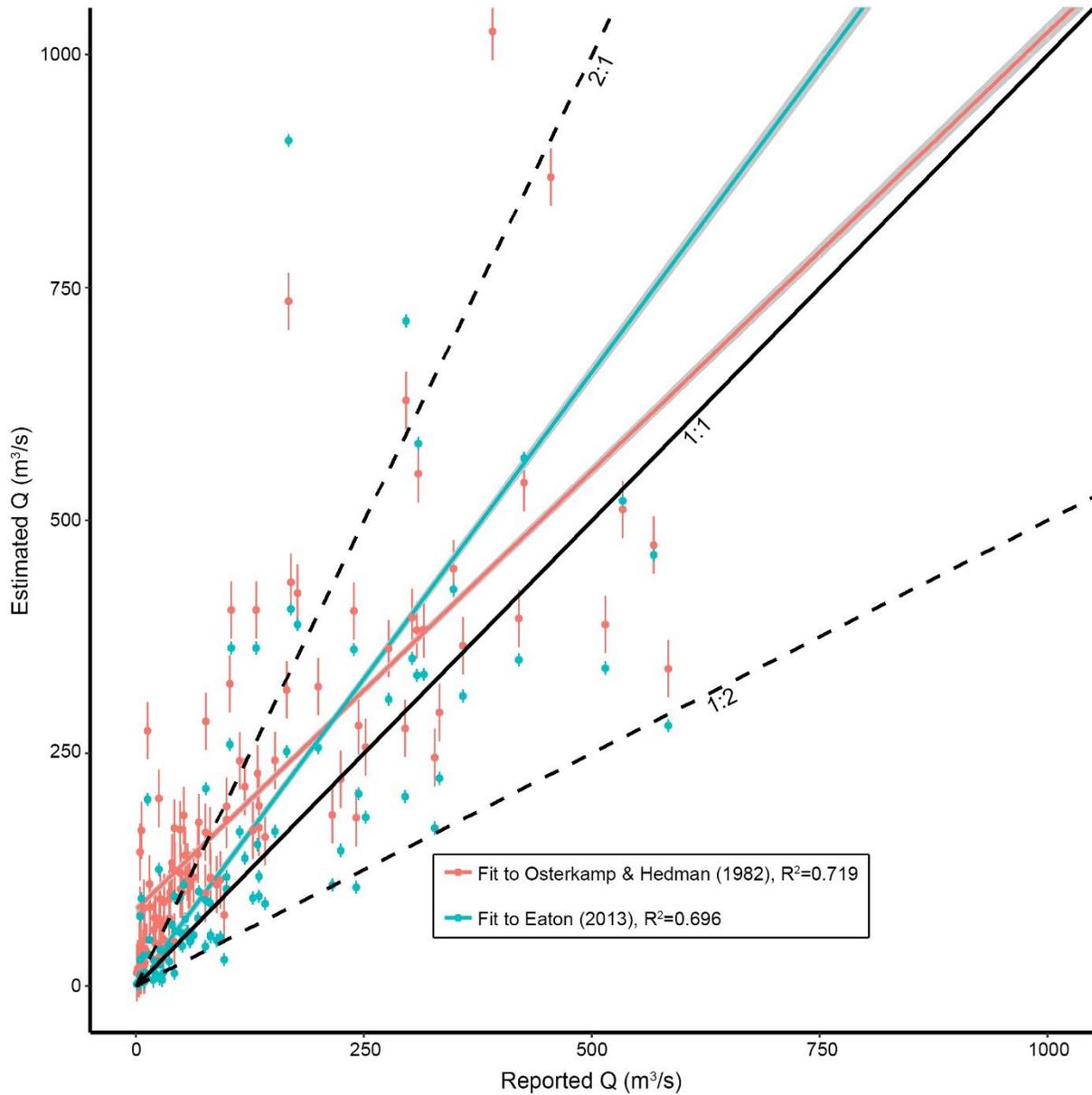
Hydraulic geometry method

267

268

269 **Figure 3.** Discharge estimate results from the threshold method, using both the field measured and DEM-derived

270 gradient. Data points shown in red and purple with error bars, and the red and purple lines indicate the locally

271 weighted regression (loess) with 95% confidence intervals. Field-measured grain size distributions were only

272 available for the smaller channels, these are apparent in the zoomed in (b). To apply the threshold approach to the

273 entire dataset, we used a grain size range of 4-64 mm.
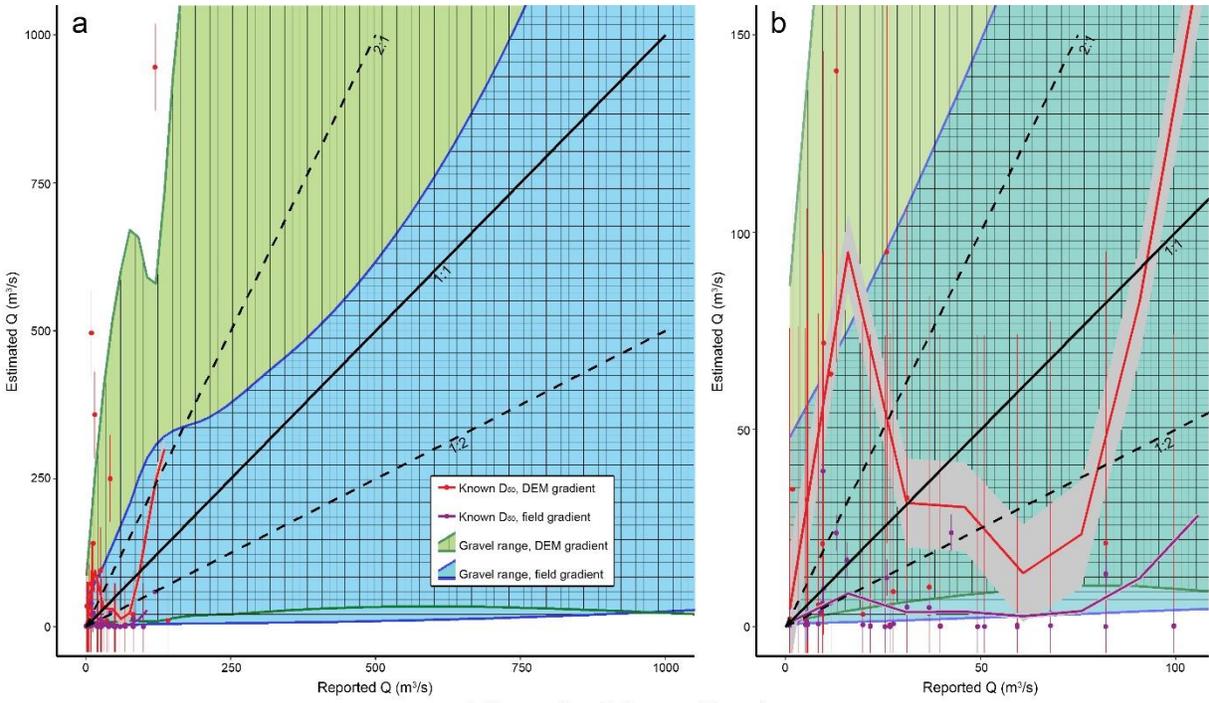
Threshold method

274

275

276 **Figure 4.** Large boulders in the Truckee River, Nevada as seen in Google Earth and Google Street View (inset,

277 looking downstream). Using these boulders as input grain sizes for the threshold approach (similar to as has been

278 done for Mars) results in unrealistically high discharges.

279

280

281

282 **References**

283 ArcGIS Online World Imagery basemap. Sources: Esri, DigitalGlobe, GeoEye, i-cubed, USDA FSA, USGS, AEX,

284   Getmapping, Aerogrid, IGN, IGP, swisstopo, and the GIS User Community

285 Barnhart, C. J., Howard, A. D., & Moore, J. M. (2009). Long-term precipitation and late-stage valley network

286   formation: Landform simulations of Parana Basin, Mars. *Journal of Geophysical Research*, *114*(E1).

287   https://doi.org/10.1029/2008JE003122

288 Castro, J. M., & Jackson, P. L. (2001). Bankfull discharge recurrence intervals and regional hydraulic geometry

289   relationsyhips: patterns in the Pacific Northwest, USA. *Journal of the American Water Resources Association*,

290   *37*(5), 1249–1262. https://doi.org/10.1111/j.1752-1688.2001.tb03636.x

291 Copeland, R. R., Biedenharn, D. S., & Fischenich, J. C. (2000). Channel-Forming Discharge. *U.S. Army Corps of*

292   *Engineers Technical Note ERDC/CHL CHETN-VIII-5*.

293 Craddock, R. A., & Howard, A. D. (2002). The case for rainfall on a warm, wet early Mars. *Journal of Geophysical*

294   *Research*, *107*(E11). https://doi.org/10.1029/2001JE001505

295 Dietrich, W. E., Palucis, M. C., Williams, R. M. E., Lewis, K. W., Rivera-Hernandez, F., & Sumner, D. Y. (2017).

296   Fluvial Gravels on Mars. In D. Tsutsumi & J. B. Laronne (Eds.), *Gravel-Bed Rivers* (pp. 755–783).

297   Chichester, UK, UK: John Wiley & Sons, Ltd. https://doi.org/10.1002/9781118971437.ch28

298 Dutnell, R. C. (2000). *Development of Bankfull Discharge and Channel Geometry Relationships for Natural*

299   *Channel Design in Oklahoma Using a Fluvial Geomorphic Approach*. University of Oklahoma, Norman,

300   Oklahoma.

301 Eaton, B. C. (2013). Hydraulic Geometry: Empirical Investigations and Theoretical Approaches. In E. (Ed. .

302   Shroder, J. (Editor in Chief), Wohl (Ed.), *Treatise on Geomorphology* (Vol. 9, Fluvial, pp. 313–329). San

303   Diego, CA: Academic Press. https://doi.org/10.1016/B978-0-12-374739-6.00243-8

304 Ehlmann, B. L., Mustard, J. F., Murchie, S. L., Bibring, J.-P., Meunier, A., Fraeman, A. A., & Langevin, Y. (2011).

305   Subsurface water and clay mineral formation during the early history of Mars. *Nature*, *479*(7371), 53–60.

306   https://doi.org/10.1038/nature10582

307 Ferguson, R. (2007). Flow resistance equations for gravel- and boulder-bed streams. *Water Resources Research*,

308   *43*(5), 1–12. https://doi.org/10.1029/2006wr005422

309 Howard, A. D., Moore, J. M., Irwin, R. P., Dietrich, W. E., Irwin, R. P., Dietrich, W. E., et al. (2007). Boulder

transport across the Eberswalde delta. In *Lunar and Planetary Science Conference 38* (p. 1168).

https://doi.org/0.1029/2005JE002460

Irwin, R. P., Craddock, R. A., & Howard, A. D. (2005). Interior channels in Martian valley networks: Discharge and

runoff production. *Geology*, *33*(6), 489. https://doi.org/10.1130/G21333.1

Irwin, R. P., Craddock, R. A., Howard, A. D., & Flemming, H. L. (2011). Topographic influences on development

of Martian valley networks. *Journal of Geophysical Research*, *116*(E2), E02005.

https://doi.org/10.1029/2010JE003620

Jacobsen, R. E., & Burr, D. M. (2016). Greater contrast in Martian hydrological history from more accurate

estimates of paleodischarge. *Geophysical Research Letters*, *43*(17), 8903–8911.

https://doi.org/10.1002/2016GL070535

Kite, E. S., Howard, A. D., Lucas, A., & Lewis, K. W. (2015). Resolving the era of river-forming climates on Mars

using stratigraphic logs of river-deposit dimensions. *Earth and Planetary Science Letters*, *420*, 55–65.

https://doi.org/10.1016/j.epsl.2015.03.019

Kite, E. S., Mayer, D. P., Wilson, S. A., Davis, J. M., Lucas, A. S., & de Quay, G. S. (2019). Persistence of intense,

climate-driven runoff late in Mars history. *Science Advances*, *5*(3). https://doi.org/10.1126/sciadv.aav7710

Kleinhans, M. G., van de Kasteele, H. E., & Hauber, E. (2010). Palaeoflow reconstruction from fan delta

morphology on Mars. *Earth and Planetary Science Letters*, *294*(3–4), 378–392.

https://doi.org/10.1016/j.epsl.2009.11.025

Konsoer, K. M., Leroy, J., Burr, D., Parker, G., Jacobsen, R., & Turmel, D. (2018). Channel slope adjustment in

reduced gravity environments and implications for Martian channels. *Geology*, *46*(2), 183–186.

Lamb, M. P., Dietrich, W. E., & Venditti, J. G. (2008). Is the critical Shields stress for incipient sediment motion

dependent on channel-bed slope? *Journal of Geophysical Research*, *113*(May 2007), 1–20.

https://doi.org/10.1029/2007JF000831

Lawlor, S. M. (2004). Determination of Channel-Morphology Characteristics, Bankfull Discharge, and Various

Design-Peak Discharges in Western Montana. *U.S. Geological Survey*, (Scientific Investigations Report 2004-

5263). https://doi.org/10.3133/sir20045263

Leopold, L. B., & Maddock, T. (1953). *The Hydraulic Geometry of Stream Channels and Some Physiographic*

Implications. Washington, D.C.: U.S. Government Printing Office. https://doi.org/10.3133/pp252

338   Luo, W., Cang, X., & Howard, A. D. (2017). New Martian valley network volume estimate consistent with ancient

339   ocean and warm and wet climate. *Nature Communications*, *8*, 1–7. https://doi.org/10.1038/ncomms15766

340   Malin, M. C., Bell, J. F., Cantor, B. A., Caplinger, M. A., Calvin, W. M., Clancy, R. T., et al. (2007). Context

341   Camera Investigation on board the Mars Reconnaissance Orbiter. *Journal of Geophysical Research*, *112*(E5),

342   E05S04. https://doi.org/10.1029/2006JE002808

343   Matsubara, Y., Howard, A. D., & Gochenour, P. J. (2013). Hydrology of early Mars: valley network incision.

344   *Journal of Geophysical Research: Planets*, *118*(April). https://doi.org/10.1002/jgre.20081

345   McEwen, A. S., Eliason, E. M., Bergstrom, J. W., Bridges, N. T., Hansen, C. J., Delamere, W. A., et al. (2007).

346   Mars Reconnaissance Orbiter's High Resolution Imaging Science Experiment (HiRISE). *Journal of*

347   *Geophysical Research*, *112*(E5), E05S02. https://doi.org/10.1029/2005JE002605

348   Moody, T., Wirtanen, M., & Yard, S. N. (2003). *Regional Relationships for Bankfull Stage in Natural Channels of*

349   *the Arid Southwest*. Retrieved from http://naturalchanneldesign.com/wp-content/uploads/2014/01/Arid-SW-

350   Report.pdf

351   Morgan, A. M., Howard, A. D., Hobley, D. E. J., Moore, J. M., Dietrich, W. E., Williams, R. M. E., et al. (2014).

352   Sedimentology and climatic environment of alluvial Fans in the martian Saheki crater and a comparison with

353   terrestrial fans in the Atacama Desert. *Icarus*, *229*, 131–156. https://doi.org/10.1016/j.icarus.2013.11.007

354   Osterkamp, W. R., & Hedman, E. R. (1982). Perrenial-Streamflow Characteristics Related to Channel Geometry and

355   Sediment in Missouri River Basin. *U.S. Geological Survey Professional Paper*, *1242*.

356   Palucis, M. C., Dietrich, W. E., Hayes, A. G., Williams, R. M. E., Gupta, S., Mangold, N., et al. (2014). The origin

357   and evolution of the Peace Vallis fan system that drains to the Curiosity landing area, Gale Crater, Mars.

358   *Journal of Geophysical Research: Planets*, *119*(4), 705–728. https://doi.org/10.1002/2013JE004583.Received

359   Parker, G. (2008). 3 - Transport of Gravel and Sediment Mixtures. In M. H. García (Ed.), *Sedimentation*

360   *Engineering - Processes, Measurements, Modeling, and Practice* (pp. 165–251). Reston, VA: American

361   Society of Civil Engineers. https://doi.org/10.1061/9780784408148.ch03

362   Parker, G., Wilcock, P. R., Paola, C., Dietrich, W. E., & Pitlick, J. (2007). Physical basis for quasi-universal

363   relations describing bankfull hydraulic geometry of single-thread gravel bed rivers. *Journal of Geophysical*

364   *Research*, *112*. https://doi.org/10.1029/2006JF000549

365   Prancevic, J. P., Lamb, M. P., & Fuller, B. M. (2014). Incipient sediment motion across the river to debris-flow

366   transition. *Geology*, *42*(3), 191–194. https://doi.org/10.1130/G34927.1

367   Presley, M. A., & Craddock, R. A. (2006). Thermal conductivity measurements of particulate materials: 3. Natural

368   samples and mixtures of particle sizes. *Journal of Geophysical Research*, *111*(E9), E09013.

369   https://doi.org/10.1029/2006JE002706

370   United States Army Corps of Engineers (2016) 2016 National Inventory of Dams, Alexandria, VA.

371   http://nid.usace.army.mil/

372   United States Geological Survey (2013). The National Hydrography Dataset (NHD). U.S. Geological Survey,

373   Reston, Virginia. https://www.usgs.gov/core-science-systems/ngp/national-hydrography/national-

374   hydrography-dataset

375   Wang, Y., & Wu, B. (2016). Comparison and co-registration of DEMs generated from HiRISE and CTX images.

376   *ISPRS - International Archives of the Photogrammetry, Remote Sensing and Spatial Information Sciences*,

377   *XLI-B4*(July), 511–517. https://doi.org/10.5194/isprs-archives-XLI-B4-511-2016

378   Williams, G. P. (1988). Paleofluvial estimates from dimensions of former channels and meanders. In R. Baker, R. C.

379   Kochel, & P. C. Patton (Eds.), *Flood geomorphology* (pp. 321–334). New York: John Wiley.

380   Williams, R. M. E., Grotzinger, J. P., Dietrich, W. E., Gupta, S., Sumner, D. Y., Wiens, R. C., et al. (2013). Martian

381   Fluvial Conglomerates at Gale Crater. *Science*, *340*(6136), 1068–1072.

382   https://doi.org/10.1126/science.1237317

383   Wilson, L., Ghatan, G. J., Head, J. W., & Mitchell, K. L. (2004). Mars outflow channels: A reappraisal of the

384   estimation of water flow velocities from water depths, regional slopes, and channel floor properties. *Journal of*

385   *Geophysical Research: Planets*, *109*(E9), E09003. https://doi.org/10.1029/2004JE002281

386   Wordsworth, R. D., Kerber, L., Pierrehumbert, R. T., Forget, F., & Head, J. W. (2015). Comparison of "warm and

387   wet" and "cold and icy" scenarios for early Mars in a 3-D climate model. *Journal of Geophysical Research:*

388   *Planets*, *120*(6), 1201–1219. https://doi.org/10.1002/2015JE004787

389

390